Astron. Astrophys. 331, 1070–1077 (1998)

ASTRONOMY
AND
ASTROPHYSICS

High velocity gas and dust evolution in Chamaeleon clouds⋆

Cecile Gry[1], François Boulanger[2], Edith Falgarone[3], Guillaume Pineau des Forêts[4], and James Lequeux[5]

[1] Laboratoire d'Astronomie Spatiale, B.P. 8, F-13376 Marseille cedex 12, France
[2] Institut d'Astrophysique Spatiale Université Paris Sud, Bâtiment 121, F-91405 Orsay, France
[3] Radioastronomie Millimétrique, Ecole Normale Supérieure, 24 Rue Lhomond, F-75005 Paris, France
[4] DAEC, Observatoire de Paris, F-92195 Meudon Principal, France
[5] Observatoire de Paris, 61 Avenue de l'Observatoire, F-75014 Paris, France

Received 6 September 1996 / Accepted 7 October 1997

Abstract. We report on GHRS observations which reveal conspicuous differences in the absorption spectra of two nearby stars, close to each other. The star HD102065 lies behind a cloud in Chamaeleon with unusually strong mid–IR emission, indicating a large abundance of very small dust particles. Along this line of sight, 5% of the gas (about 6 10^{19} cm^{-2}) is at large velocities (up to -50 km s^{-1}) compared to the main absorption component at v_{lsr} $\sim$0 km s^{-1}. The high velocity gas is very excited and has an unusually large silicon abundance. The other star HD96675 lies behind a cloud with standard mid–IR emission. Along this line of sight, high velocity gas is also detected, but to somewhat smaller offset velocities and with a much lower excitation. In particular, the SiII* lines are not observed.

From the excitation of Si^+ and C^+ in the direction of HD102065, we infer that the high velocity gas has a temperature higher than several 100 K and an electron density of at least 10 cm^{-3}. These results, together with the lack of an ionizing star in the neigborhood, suggest that a large amount of kinetic energy is being deposited in this gas. The collision of an infalling cloud and a local cloud is a plausible source of energy. The peculiarity of the dust size distribution inferred from the IRAS data is likely to be related to the processes which dissipate the kinetic energy and heat the gas. A shock seems to be required to produce the excitation and ionization degrees. But the carbon ionization ratio combined with the electron density inferred from the silicon and carbon excitation implies that carbon is not in ionization equilibrium and should recombine extremely quickly. Future higher resolution observations might help solving this incoherency.

Key words: ISM: Chamaeleon clouds – stars: HD 96675; HD 102065 – ISM: atoms; kinematics and dynamics – shocks

1. Introduction

IRAS images of nearby clouds have disclosed large variations, even at small scales, in some of the colors of their dust emission (Boulanger et al. 1990). The 12 μm/100 μm ratio, in particular, is observed to be very large in well–defined regions, and this is due to an excess emission of the dust in the mid–IR. This excess emission has been correlated with changes in the shape of the UV part of the extinction curve for a sample of stars located behind nearby clouds in Chamaeleon (Boulanger et al. 1994), suggesting that it is the small size tail of the size distribution of grains which is responsible for the 12 μm/100 μm color variations. Indeed, models of the IR emission of interstellar clouds show that the observed mid–IR excesses trace an overabundance of the very small particles emitting in the mid-IR (sizes in the range 10 to 35 Å) by more than one order of magnitude from cloud to cloud and within clouds (Bernard et al. 1993). A process is therefore effective in populating the small size tail of the dust distribution, in those regions of intense mid–infrared emission. Recent work suggests that the shattering of grains in grain–grain collisions is an efficient process to grind down interstellar grains to very small sizes. The effect of this process on the grain size distribution has only been investigated in fast shocks (100 km s^{-1} and higher) propagating in low density gas (Jones et al. 1996) but it is predicted to be effective for lower velocities and in denser gas, considering the low velocity threshold of the shattering process.

Whatever it might be, the process driving the dust evolution is expected to have observable signatures in the gas. To look for such signatures, we have conducted a spectroscopic study in the visible range of the gas along the same lines of sight for which UV extinction curves had been obtained. These stars are all within an 8 square degrees field, are all nearby stars (d<400 pc) located not far beyond the Chamaeleon complex which has an estimated distance of 150 pc (Boulanger et al. 1994). For all lines of sight, the detection of CH suggests that the absorbing gas is molecular to a significant extent. Gas along the lines of sight with intense mid-IR emission stands out for having

⋆ Based on observations with the NASA/ESA *Hubble Space Telescope,* obtained at the Space Telescope Institute, which is operated by the Association of Universities for Research in Astronomy, Inc., under NASA contract NAS5-26555.

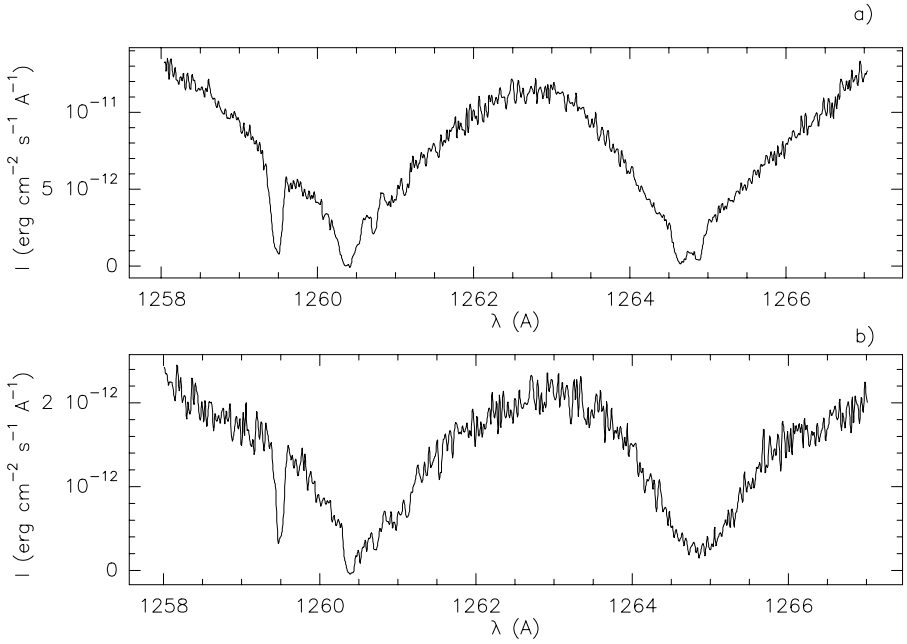

Fig. 1a and b. GHRS-G160M spectra of the stars HD102065 **a** and HD96675 **b**. One of the SII lines (1259.5 Å), the SiII line (1260.4 Å), the CI line (1260.7 Å) and several excited CI lines (between 1260.9 Å and 1261.5 Å) are visible in the two spectra. An FeII line (1260.5 Å) is blended with the broad SiII line in the spectrum of HD102065. The doublet absorption from the excited fine structure level of SiII (1264.7 and 1265.0 Å) is seen only in the direction of HD102065.

Table 1. GHRS observations used in the analysis

grating	aper	range (Å)	spectral lines and wavelengths (Å)
G160M	SSA	1249-1282	SII 1250, 1253, 1259, SiII 1260, SiII* 1265, CI 1270, 1277 (multiplets), CO 1263, CO 1281
G160M	SSA	1321-1356	CI 1329 (multiplet), CII 1334, CII* 1335, CO 1322, CO 1344
G160M	SSA	1445-1480	CO 1447, CO 1477, SI 1472

a high abundance of CH^+, a molecule which forms from the reaction of C^+ and H_2, only where the endothermicity of the reaction (T=4650 K) is overcome (Boulanger 1994). The detailed results of these observations will be reported in a companion paper, with additional results on molecular line emission of the Chamaeleon clouds (Boulanger et al. in prep.). Among the sample of stars observed in the visible range, we selected two stars 4.6° apart from each other – HD 96675 and HD 102065 – for further study with the GHRS-G160M spectrometer on board of the HST. HD 102065 is located behind a cloud with exceptionally bright 12 μm and 25 μm emission with respect to its 100 μm emission. The mid–IR emission is substantially fainter for HD 96675 while the far–IR emission is comparable. Both stars have had their distance measured by Hipparcos and hence their luminosity class confirmed: 168 pc for HD102065 and 164 pc for HD96675. Note that the star distances are included in the estimated distance ranges for the Chamaeleon complex (e.g. Corradi et al. 1997; Whittet et al. 1997). This supports the idea that the gas observed in absorption in these lines of sight is either local or associated with the Chamaeleon clouds. In Sect. 2, we describe the observations and the main differences observed in the spectra along each line of sight, namely the clear differences of excitation for the lines in each velocity interval. In Sect. 3, we discuss the characteristics of the gas at high velocity. In Sect. 4, we investigate the possible interpretations and the implications of these observations and propose a possible link of the components at high and low velocities, involving the collision of a high velocity cloud upon a local cloud.

2. Observations and processing

We have performed GHRS observations of several interstellar lines from elements characteristic of the neutral and slightly ionized phases of the interstellar medium. The observations were carried out during the Ech-A disability of Cycle 2 and we observed three wavelength set-ups of the G160M grating leading an intermediate resolution around 20 000. The observations are listed in Table 1 together with a list of the lines used in each domain. We used the 0.25″ small science aperture (SSA), the procedure FP-SPLIT = 4 and a sub-stepping of two samples per diode width (for details on instrumentation see Duncan 1992). The data have been processed with the standard STSDAS procedures in the IRAF software. Wavelengths were assigned from standard calibration tables. Because of magnetic drift effects one can expect wavelength assignment errors as large as ± 1 resolution element. For this reason our data do not give absolute velocities and we have assigned the zero velocity by assuming that the CI and SI lines have the same central velocity as the molecular lines of CO observed from the ground. This assumption seems reasonable as the corrections never exceed 1 resolution element. Based on this assumption, we can assign a relative velocity to all species studied here. The main difference between the two lines of sight is clearly visible in the spectra

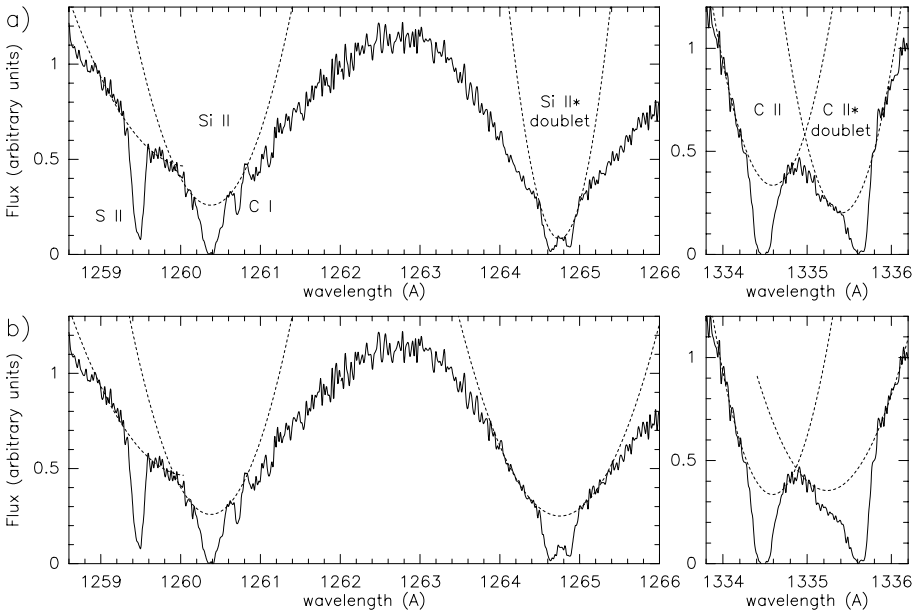

Fig. 2a and b. Observed absorption profiles for SiII and CII in the line of sight of HD 102065. Si II* and C II* denote the doublets from the excited fine structure levels. The upper plots (Fig. 2a) show the adopted stellar profiles used to normalize the spectra. The lower plots (Fig. 2b) show for the two excited species alternative shallower stellar profiles which would have led to an even stronger interstellar contribution in these lines.

displayed in Fig. 1: the SiII lines are seen on the two lines of sight, while absorption from the excited fine structure level of Si^+ is seen only in front of HD102065.

The first difficulty in the data reduction lies in the separation of the stellar absorption from broad interstellar absorption lines. We derive a stellar profile by fitting a 2^{nd} order polynomial in the vicinity of the interstellar absorption. The difficulty which sometimes occurs in this process is illustrated in Fig. 2 where we show two solutions that bracket the widths and intensities of the stellar absorption profiles. Fig. 2a shows the adopted C^+ and Si^+ stellar profiles. Fig. 2b shows alternative solutions for the CII* and SiII* stellar absorptions, which are at least as conceivable. In the following, for the interpretation of the excited line profiles, we adopt the deepest possible stellar profiles (Fig. 2a) to make sure that our derived lower limits on the excitation ratios are the lowest permitted by the observed spectrum, i.e. that the most conservative solution is considered. The resulting SII, CII, CII*, SiII and SiII* absorption lines, once normalized to a stellar continuum equal to unity, are shown in Fig. 3. The SII, CII, and CII* spectra of both stars, HD 96675 and HD102065, are superimposed on the same velocity scale. When appropriate to analyse the interstellar absorption, we use a line profile fitting program where the absorption line is represented by a theoretical Voigt profile convolved with the GHRS instrumental profile taken from Duncan (1992).

3. Characteristics of the gas

3.1. Low velocity gas

The optical and infrared characteristics of each line of sight are given in Table 2. The visual extinction values taken from Boulanger et al. (1994) are used to derive the total hydrogen column densities from the standard $N(H)/A_v$ ratio ($N(H)/A_v$ = 1.86×10^{21} cm^{-2}). The bulk of the gas along the two lines of sight appears in a low velocity component at $v_{lsr} \sim -3$ km s^{-1}. The analysis of the neutral species (CO, CH and CI) is discussed in Boulanger et al. (1998, in prep.), as well as that of the CH^+ radical, also observed in one single component at $v_{lsr} = -3$ km s^{-1}. In Table 2, we list the column densities of these species observed at low velocity to further characterize the two lines of sight: the CH^+ radical is twice as abundant as CH along the line of sight to HD 102065 but is only $\sim$ 10% of CH in the direction of HD 96675. Note also that there is a large difference in CO abundance between the two lines of sight. The ion lines SII, SiII and CII are all saturated at low velocity, making it difficult to determine reliable column densities (see for example the comparison of the three SII absorption lines in Fig. 3).

Table 2. Visible and infrared characteristics of the sight-lines and column densities of molecular and neutral atomic species at **low velocity**

Line of sight	HD 96675	HD 102065
α(2000)	11 05 58.17	11 43 37.87
δ(2000)	-76 07 49.0	-80 28 59.4
spectral type	B7V	B9IV
A_V (mag)	1.1 $\pm$0.15	0.67 $\pm$0.12
d (pc)(Hipparcos)	164	168
$I_{12\mu}$ (MJy sr^{-1})	0.4 ± 0.1	0.75 ± 0.1
$I_{100\mu}$ (MJy sr^{-1})	9.6 ± 0.5	7.0 ± 0.5
N(H) (cm^{-2})	2.0 10^{21}	1.2 10^{21}
N(CH) (cm^{-2})	2.2 10^{13}	6.3 10^{12}
N(CH^+) (cm^{-2})	2.8 10^{12}	1.2 10^{13}
N(CO) (cm^{-2})	$> 10^{15}$	(7 ± 3) 10^{13}
N(CI) (cm^{-2})	> 1.7 10^{15}	(4 ± 1) 10^{14}
N(CI*) (cm^{-2})	> 2 10^{14}	(8 ± 2) 10^{13}
N(CI**) (cm^{-2})	4.6 10^{13}	$(1.8 \pm .4)$ 10^{13}

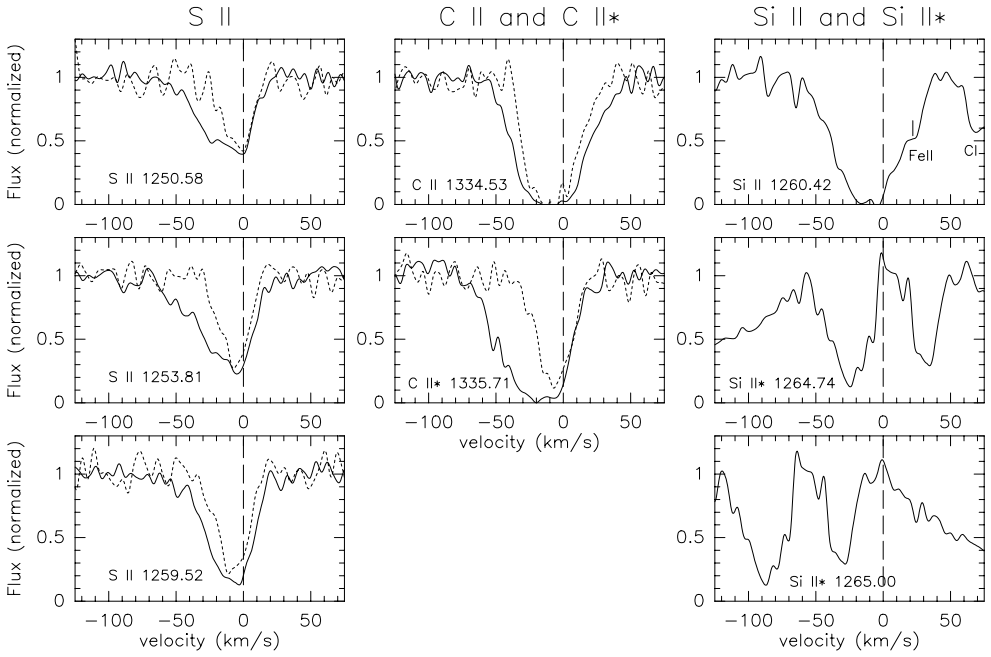

Fig. 3. Normalized interstellar profiles shown as a function of velocity. The normalization for the excited species has been performed with the deepest possible stellar absorption profiles as shown in Fig. 2a. This minimizes the interstellar absorption in these species. The doublet SiII* is shown successively in the velocity frame of both lines. For the CII and SII lines, the spectrum of HD96675 (dashed line) is superimposed on that of HD102065. This illustrates the velocity distribution difference between the two lines of sight. Note also that toward HD102065 the lines from the excited levels CII* and SiII* are centered at a more negative velocity than the lines from the ground state.

3.2. Column densities of the high velocity gas

The important result of the GHRS observations is the detection of gas at large negative velocities. The SII and CII absorption lines along the two lines of sight are compared in Fig. 3. Two salient features of the profiles appear on this figure. First, for both lines of sight, interstellar absorption extends to large negative velocities in addition to the low velocity component. But the SII absorption lines reveal that the amount of gas at negative velocities is smaller for the star HD96675 where it extends to $\sim$ -25 km s^{-1} compared to -50 km s^{-1} for the star HD 102065. Second, the absorption in the excited CII* line is much larger toward HD102065 than toward HD96675. Together with the lack of the SiII* absorption in the direction of HD96675 (Fig. 1), these results suggest that the excitation conditions in the high velocity gas along the two lines of sight are very different. In addition, absorption lines from the excited species CII* and SiII* toward HD102065 (Fig. 3) are shifted towards more negative velocities than those from the ground states.

We investigate below the various species column densities in the high velocity gas toward the star HD102065.

For all ions the absorption is continuous from v_{lsr} = 0 up to the extreme velocities and at the present resolution it is unclear if the high velocity absorption is produced by gas spread continuously in velocity or by a set of discrete velocity components. It is therefore difficult to perform a detailed fitting of the profiles which requires the assumption of a gas velocity distribution.

Furthermore it is visible that the lines are saturated even at high velocity: the optical depths of the three sulfur lines are not in the ratios of their oscillator strengths, i.e 1:2:3.

For SII, we thus derive a lower limit on the column density of $5\,10^{14}$ cm^{-2}, which corresponds to the optically thin limit for the weakest of the lines. As we have three lines with a difference of a factor of 3 in the f-values, the constraint of having to find a good fit simultaneously in the three lines allows the determination of a unique set of parameters (N, b, v_{lsr}) in the case of a single component. In the spectrum of HD102065, the simultaneous fit of the high velocity part of the three SII lines with one component implies a column density of N(SII) = 1.1 $\pm$.2 10^{15} cm^{-2}, centered at v_{lsr} = -23$\pm$ 1 km s^{-1} with a Doppler parameter b=4.5$\pm$.5 km s^{-1}. In the following we will adopt this value for N(SII), keeping in mind that the strict lower limit is lower by a factor of two, which would not alter the conclusions of the paper.

We derive an estimate of the total column density of high velocity gas from the SII column density and the sulfur solar abundance ($\log(S/H)_\odot$=-4.73) by making the common assumption that sulphur is undepleted and almost fully ionized in low column density gas due to its low ionization threshold (10.36 eV): N(H) = 6 $\pm$ 1 10^{19} cm^{-2}. A similar column density is derived from the HI data of Cleary et al. (1979) which, at the positions of both stars, shows HI emission over the same range of velocities as observed in interstellar absorption. The comparison of the HI and total hydrogen column densities indicates that the molecular fraction of the high velocity gas in the direction of both stars is small.

If we try to fit the high velocity part of the SiII 1260 Å line in the HD102065 spectrum with a component at the same velocity and with same b-value as the SII lines, the fit implies a Si^+ column density which involves the total silicon cosmic abundance, as if all the silicon in the high velocity component of this line of sight had returned to the gas phase. This is unusual since, unlike sulphur, silicon is usually depleted in the interstellar medium, with only about 5% of the silicon in the gas phase in the cool disk matter and 40% in the warm disk (Savage and Sembach 1996) and a minimum depletion of about -0.15 dex for the high velocity clouds in the halo (Fitzpatrick, 1996). However, the

Table 3. Column densities for the **high velocity** gas in the line of sight to HD 102065. The mention 'measured' indicates that the column density has been derived from the profile with the help of a fitting procedure; 'from SII' indicates that the value is derived from N(SII) with the assumption of cosmic abundances.

High velocity gas	cm^{-2}
N(SII) (measured)	$\sim 1.1\ 10^{15}$
N(SiII*) (measured)	$> 8\ 10^{13}$
N(H) (from SII)	$\sim 6\ 10^{19}$
N(SiII) (from SII)	$\lesssim 2.1\ 10^{15}$
N(CII)+N(CII*) (from SII)	$\sim 6\ 10^{15}$
N(SiII*)/N(SiII)	$> .04$
N(CII*)/N(CII) (observed)	~ 1
N(CI) (not detected)	$< 4\ 10^{12}$
$N(CH^+)$ (not detected)	$< 3\ 10^{12}$

SiII 1260 Å line is heavily saturated so the column density that can be derived from the fit of this single line is highly uncertain. We will thus adopt the upper limit $N(Si^+) \leq 2.1\ 10^{15}$ cm^{-2} derived from $N(S^+)$ in the extreme case where there is no silicon depletion.

Spectra of the neutral atoms CI and SI do not show absorption at high velocity. We derive a 3 σ upper limit $N(CI) < 4\ 10^{12}$ cm^{-2} in this component. We have estimated the high velocity CII column density by combining the high velocity H I column density as derived from SII with a conservative gas phase abundance of carbon ([C]/[H]=10^{-4}) (Table 3). We then derive a lower limit for the carbon ionization degree CII/CI$>$ 1500.

The results for the high velocity gas are summarized in Table 3.

3.3. Excitation conditions in the high velocity gas

In the spectrum of HD102065 Si^+ is detected in its fine-structure level (414 K) in an absorption doublet (Fig. 1 and 3). From the weakest of the two lines, we derive a lower limit N(SiII*) $> 8\ 10^{13}$ cm^{-2} corresponding to the minimum column density that gives a reasonable fit when the observed profile is fitted with a single component. We find for the single component a velocity of -33 km/s and a b-value of 4.5 km/s. The column density corresponding to the optically thin limit is only slightly lower: $5\ 10^{13}$ cm^{-2}.

For the high velocity gas of total column density N(H)= $6\pm1\ 10^{19}$ cm^{-2} and a gas phase silicon abundance equal to the cosmic value, we obtain a lower limit on the excitation ratio: [SiII*]/[SiII] $> 4\ 10^{-2}$ which is quite high. Comparison of this lower limit with the calculations of Keenan et al. (1985) implies that the temperature is at least a few 100 K, whatever density is considered. It also implies that the excitation is dominated by electrons with an electron density n_e higher than 10 cm^{-3}. Neutral atoms could produce the excitation only for gas densities larger than 10^4 cm^{-3}. But this alternative solution seems unlikely since it would imply a very high gas pressure.

The straight comparison of the CII and CII* profiles toward HD102065 in Fig. 3 shows that in the high velocity wing around v_{lsr} = - 50 km s^{-1}, the abundance of CII* is comparable to and even larger than that of CII. This implies a very high excitation of the high velocity part of the CII line close to thermalisation which, when compared to calculations by Keenan et al (1986), also implies a temperature over a few 100 K and electron density slightly higher than 10 cm^{-3}, consistent with the physical conditions inferred from the Si^+ excitation.

4. Nature of the high velocity gas

4.1. Is the high velocity gas due to the stellar wind or circumstellar material?

It is very unlikely that the star HD102065 of type B9 IV has a wind powerful enough to be at the origin of the high velocity absorption features. This is corroborated by examination of the UV atlas (Snow et al.,1994) which includes B9 stars down to luminosity class III, and those stars do not show any sign of winds.

We have nevertheless considered the possibility that the high velocity gas could be swept up material forming an expanding shell around the star. Boulanger et al. (1994) pointed out that HD102065 is a faint point-like source (size smaller than 5') on the 60μm and 100μm IRAS images, which implies the presence of matter within 0.1 pc of the star. The far-IR luminosity of the source is estimated to be $4\ 10^{-2} L_\odot$ as compared to a stellar luminosity of $\sim 100 L_\odot$. From the ratio between infrared and stellar luminosity we derive an overall opacity of the matter surrounding the star of $4\ 10^{-4}$. Using an absorption opacity in the UV of $10^{-21} cm^2\ H^{-1}$, the opacity corresponds to a gas column density of $4\ 10^{17}$ cm^{-2}, more than two orders of magnitude lower than the high velocity gas column density, $6\ 10^{19} cm^{-2}$. The IRAS data thus allow to exclude the existence of a shell around HD102065 with such a high column density within 0.1 pc of the star. We conclude that the high velocity features cannot be due to the wind of the star or to material swept up by the stellar wind.

Another stellar interpretation of the data implies matter flowing within a binary system. This interpretation has been given by Trapero et al. (1996) when reporting on the detection of high velocity gas in the spectrum of the B7 III star η Tau, with the particularity that the CII* 1335 Å line is stronger than the CII 1334 Å line. But the column density we find for the high velocity gas is almost three orders of magnitude higher than the gas column density involved in the case of η Tau (they find N(H) = 10^{17} cm^{-2}). η Tau is moreover known as a binary, as opposed to HD102065.

We will thus assume in the subsequent discussion that the high velocity gas is interstellar.

4.2. Spatial distribution of high velocity gas in Chamaeleon

In the HI data of Cleary et al. (1979), the HI emission at negative velocities extends over the whole Chamaeleon field. Some of the gas seen at these negative velocities could be remote gas since it corresponds to the velocities expected from the rotation

curve of the Galaxy in this direction. But part of it must be local since it is also seen in optical absorption spectra in the direction of the two nearby stars discussed in the present paper and in the direction of a few other stars in the Chamaeleon area (Penprase, 1993). These data suggest a widespread presence of local gas at large negative velocities, spread at least over several tens of parsecs. We therefore conclude that the low and high velocity components are associated and that they both belong to the local Chamaeleon complex. This conclusion is supported by the distance to the target stars, similar to the distance to the Chamaeleon complex itself. In the case of HD 102065, the high excitation conditions suggest that there is a physical violent interaction between the two velocity components. We may be observing the interaction of infalling gas with gas in the disk. The kinetic energy in the infalling gas could be the source of energy required to explain the high excitation.

4.3. Energy supply

The strength of the SiII* absorption in the high velocity gas toward HD102065 implies that the energy radiated in the associated 35μm fine structure line of Si^+, L(35μm) $\simeq 10^{-24}$ erg s^{-1} per H nucleon. This is a factor 20 larger than the average cooling rate in the CII 158μm line of the gas in the Solar Neighborhood (Gry et al. 1992). Since the emission from other lines (OI, CII, H_2) will add to this already very large value, it is clear that a large amount of energy is being deposited in the gas and that a substantial fraction of this energy is being dissipated. Both excitations of the SiII and CII lines require an electron density $n_e \gtrsim 10$ cm^{-3}. Since the total column density is N(H)$\sim 6\,10^{19}$cm^{-2}, the gas if fully ionized would have an emission measure of 200 pc cm^{-6} and would be known as an HII region well visible in the Galactic Hα survey of Sivan (1974). Further, within and in the neighborhood of the Chamaeleon complex, there is no star able to produce such an ionization. To fully photoionize the high velocity gas, a flux of 10^8 Lyc photons s^{-1} cm^{-2} would be required. This flux is two orders of magnitude larger than the values derived from Hα observations of high latitude clouds away from HII regions (Reynolds et al. 1995).

The high velocity gas is thus partially ionized. The existence of partially ionized gas has also been proposed by Spitzer and Fitzpatrick (1993) to explain the excitation of CII along the line of sight to the halo star HD 93521. However, the electron density required here is two orders of magnitude higher. We therefore infer from the strength of the absorption lines at high velocities in the direction of HD102065 that the high velocity gas there does not have the properties of the diffuse warm ionized medium and that the energy dissipated and eventually radiated in the Si^+ fine structure line is not provided by stellar radiation.

4.4. Dust processing

The large abundance of silicon in the high velocity gas suggests that the dissipation process is energetic enough to sputter and/or shatter interstellar grains. It is probably not a mere coincidence if we observe signs of dust processing along a line of sight selected for crossing a cloud with peculiarly high mid-IR emission.

Indeed the purpose of the observations described here was originally to study the physical conditions of the gas associated with an exceptionally bright mid–infrared emission indicative of an enhanced small particles abundance.

Fragmentation of large dust grains into small particles is predicted by the models of Jones et al. (1996) of grain destruction in high velocity shocks produced by supernovae. Here the conditions are different (higher density and lower velocity) but Jones et al. suggest that the energy threshold for grain shattering is low. Sputtering of grains by heavy neutral species is also believed to be a significant destruction mechanism in MHD shocks (Field et al. 1997). The 12 μm emission in the Chamaeleon could be the result of the large scale interaction of local clouds with infalling gas, some of which could still be on-going. In this case we were fortunate enough to observe a region where the interaction has just happened or is still taking place.

4.5. Can an MHD shock account for the gas excitation and ionization?

We can compare our results regarding the gas at high velocity in the direction of HD102065 to the observations of high velocity and high excitation gas in the Vela remnant by Jenkins & Wallerstein (1995). They observed high excitation gas at a high velocity of 125 km s^{-1}. The column density of excited Si^+ they measure for this component, N(SiII*)=3 10^{11}cm^{-2} is two orders of magnitude smaller than the Chamaeleon value, while the CI column density, N(CI)=5 10^{13} cm^{-2} is much larger than our upper limit ($\sim 10^{12}$ cm^{-2}). Jenkins & Wallerstein propose that the excited gas is shocked gas in which neutral atoms like CI have already recombined.

The fact that only ionized species are detected at high negative velocities have led us to consider that the gas has been accelerated by a magnetic precursor in an MHD shock. This gas would correspond to the shock layer where no significant neutral-drag by ions has yet occurred. In this layer, the electron density could have the high value required to explain the gas excitation.

Existing models for MHD shocks in partially molecular gas do not provide large electron densities in the shock because molecular hydrogen there rapidly reacts with C^+ to form molecular ions like CH^+, CH_2^+ and CH_3^+ which in turn rapidly recombine with electrons. At the high velocity of the shock (50 km/s or more), the electron temperature should be sufficiently high to dissociate molecular hydrogen via excitation of the Lyman and Werner transitions (Aiello et al. 1984, Flower et al. 1996). Moreover, H_2 could also be dissociated through collisions against dust grains (Schilke et al. 1997). The shocked gas would thus be mostly atomic, in agreement with the fact that no molecular line is detected at those velocities. In such a shock, with only traces of molecular hydrogen, molecular ions cannot form and recombination with electrons is reduced. The electrons are not lost through recombination in the shocked gas and the electron density in the shock can be estimated from the amplitude of the

compression of charged species which occurs ahead of that of the neutrals due to the magnetic precursor present in shocks. The compression rate of charged species and magnetic field is roughly equal to the ratio of the shock to pre–shock velocity, and approaches two orders of magnitude for a 50 km s^{-1} shock. In a pre–shock gas of density of $n_H \sim 10^3$ cm^{-3} with ionization degree $\sim 10^{-4}$, $n_e \sim 0.1$ cm^{-3} which gives an electron density in the shocked ionized component ~ 10 cm^{-3} for the parameters chosen above. This electron density is comparable to the value imposed by the C^+ and Si^+ excitation.

An interesting consequence of a picture in which H_2 is dissociated in the shock is that CH^+ cannot form in the shocked gas. This would be consistent with the fact that CH^+ is observed only at low velocity in the line of sight toward HD 102065, as it is in all other lines of sight where it is detected. This molecule which can be formed only if the endothermicity of the C^+ + H_2 reaction is overcome might form, alternatively, in warm regions locally heated, up to $\sim 10^3$ K, by the intermittent viscous dissipation of turbulence (Falgarone & Puget 1995; Falgarone, Pineau des Forêts & Roueff 1995). If the shock is due to the collision of an infalling gas cloud on to a local cloud at low velocity, supersonic turbulence might be generated in the unstable shear layers between the infalling cloud and the target cloud. The timescale for the development of turbulence in shear layers is short, of the order of the turn over timescale of the energy containing scale, say $2\,10^3$ years for a velocity shift of ~ 50 km s^{-1} across a layer of thickness 0.1 pc, which is of the same order as the shock crossing time. In such a scenario, the high velocity gas of lower excitation observed in the direction of the other star, HD96675, is infalling gas before any interaction with local clouds has yet taken place. The interpretation of our data, though, meets a major difficulty with the ionization ratio of carbon.

4.6. Problem: carbon equilibrium time-scale

The non-detection of the CI line in the high velocity gas leads to an upper limit of the CI column density $N(CI)_{HV} < 4\,10^{12} cm^{-2}$ which, combined with the CII column density derived from N(SII) in this velocity range, $N(CII)_{HV} \sim 6\,10^{15} cm^{-2}$ provides a large carbon ionization degree $n(CII)/n(CI) > 1500$.
This result combined with the electron density shows that the ionizing process for carbon is necessarily out of equilibrium. If there were equilibrium, the ionization rate ξ, whatever its origin, should satisfy the equality between the ionization and recombination rates,

$$\xi\, n(CI) = \alpha_2\, n(CII)\, n_e,$$

where $\alpha_2 = 4.4\,10^{-12}(T/300K)^{-0.61}$ cm^3 s^{-1} is the recombination rate over all levels but the fundamental. For the electron density $n_e \sim 10\,cm^{-3}$ and temperature $T > 300K$ the carbon ionization degree can be satisfied at equilibrium only for an ionizing process such that $\xi > 7\,10^{-8}$ s^{-1}. The Solar Neighborhood interstellar radiation field provides an ionization rate $I_{UV} = \Phi_{UV}\sigma\, e^{-2.5A_v} \sim 2.2\,10^{-11}$ s^{-1} for $\Phi_{UV} \sim 2\,10^7$ photons $cm^{-2}s^{-1}$ in the Solar Neighborhood in the range $1100\,Å < \lambda < 912\,Å$, $\sigma = 6\,10^{-18}$ cm^2 and $A_v = 0.67^m$. The ratio between far-IR emission and visible extinction in the line of sight shows that there is no additional UV source (Boulanger et al. 1994). Other ionization processes like cosmic rays or high speed collisions between carbon atoms and dust grains are less efficient.

The difficulty thus lies in the following: in the absence of any competitive ionization process, the elapsed time from a fully ionized condition for carbon is given by

$$\tau = -n(CI) \,/\, [dn(CI)/dt] = 1 \,/\, [\alpha_2 \times n_e \times n(CII)/n(CI)]$$

which with our estimates of n_e and n(CII)/n(CI) gives $\tau \leq 1.5\,10^7$s. This is an implausibly short time scale which raises a puzzling problem for any explanation of the data.
In the assumption of a shock, the shock velocity of 50 km/s implies that the thickness of the layer where accelerated CII ions have not yet recombined should be less than $3\,10^{14}$ cm. For the high velocity CII column density of $6\,10^{15}\,cm^{-2}$, this implies a carbon density of $25\,cm^{-3}$, very close to the electron density. Such a layer may well exist but the puzzling question is why do not we see any downstream gas where the ions have already recombined?

When deriving estimates of physical conditions, we had to assume that the high velocity gas is somehow homogeneous and that it is justified to relate the column density derived from SII, which samples the bulk of the high velocity gas, with the column density derived from the excited species SiII* and CII*. As the observation profiles show that the excited species velocities are displaced towards more negative values than those from the ground-states, this assumption might not be totally correct. But as noted in Sect. 3, the resolution of the present data do not allow to investigate the velocity distribution of the different species. Observations with higher velocity resolution could uncover relevant variations of physical conditions with gas velocity.

5. Conclusions and perspectives

We have presented the results of UV spectroscopy in the direction of two nearby stars of the Chamaeleon complex, which have been selected on the basis of the very different mid–infrared properties of the dust lying along their lines of sight. The observations have revealed a number of unexpected results:
– the existence of gas at high negative velocities in the direction of both stars, up to $v_{lsr} \sim -50$ km s^{-1} in the direction of HD102065. This result, combined with other data in the same complex, suggests the existence of widespread nearby gas at large negative velocities in the Chamaeleon region.
– the excitation of the ion lines is large only in the direction of HD102065, which is the line of sight with the large mid–infrared emission. The high excitation of C^+ and Si^+ implies an unusually high electron density, $n_e \sim 10$ cm^{-3} given the lack of ionizing source in the vicinity.
– the silicon gas phase abundance in the high velocity gas toward HD102065 is close to the cosmic abundance.

The energy radiated by the high velocity gas in the 35 μm Si^+ line, inferred from the column density of excited ions, is very high and we suggest that a large amount of kinetic energy

is being supplied by a large scale infall of gas.

The constraints induced by the analysis of the observations has led us to consider an interpretation that involves a shock produced by the interaction of local gas with infalling gas. This interpretation has interesting consequences regarding the processing of interstellar grains and the formation of the CH^+ molecule.

However the non-detection of CI at high velocity combined with the derived CII column density implies too high an ionization ratio for carbon which should recombine very quickly at the inferred electron density. This apparent inconsistency might be related to small scale inhomogeneities in the physical conditions, if those vary with velocity. In the near future we will get higher resolution ($R \sim 100\,000$) spectra of HD102065 with STIS on board of the HST. They will help pointing out heterogeneous conditions in the high velocity gas. Only with them can we assess the full significance of the phenomenon evidenced by our data.

Acknowledgements. We are grateful to our anonymous referee for his/her comments that triggered substantial improvements in the discussion and in particular for pointing out the time-scale problem with the carbon ionization. We also acknowledge fruitful discussions with D. Flower.

References

Aiello J.M., Shemansky D., Kwok T.L., Yung Y.L. 1984, Phys. Rev. A 29, 636
Bernard J.P., Boulanger F., Puget J.L. 1993, A&A 277, 609
Boulanger F., 1994, in The First Symposium on the Infrared Cirrus and Diffuse Interstellar Clouds, eds. R.M. Cutri and W.B. Latter, p. 101
Boulanger F., Falgarone E., Puget J.L., Helou G. 1990, ApJ 364, 136
Boulanger F., Prévot M.L., Gry C. 1994, A&A 284, 956
Cleary M.N., Heiles C., Haslam C.G.T., 1979, A&AS 36, 95
Corradi W.J.B., Franco G.A.P., Knude J., A&A, 1997, in press
Duncan D, 1992, Goddard High Resolution Spectrograph Instrument Handbook, version 3.0, Space Telescope Science Institute.
Falgarone E., & Puget J.–L., 1995 A&A 293 840
Falgarone E., Pineau des Forêts G., Roueff E., 1995 A&A 300 870
Field D., May P.W., Pineau des Forêts G., Flower D.R., 1997, MNRAS 285, 839
Fitzpatrick E.L., 1996, ApJ 473, L55
Flower D.R., Pineau des Forêts G., Field D., May P.W. 1996, MNRAS 280, 447
Gry C., Lequeux J., & Boulanger F., 1992, A&A 266, 457
Jenkins E.B. & Wallerstein G., 1995, ApJ 440, 227
Jones A.P., Tielens A.G.G.M., Hollenbach D.J., McKee, C.F. 1996 ApJ 469, 740
Keenan F.P., Johnson C.T., Kingston A.E., Dufton P.L, 1985, MNRAS 214, 37p
Keenan F.P., Lennon D.J., Johnson C.T., Kingston A.E., 1986, MNRAS 220, 571
Penprase B.E. 1993, ApJS 88, 433
Reynolds R.J., Tufte S.L., Kung D.T., Mc Cullough P.R., Heiles C., 1995, ApJ 448, 715
Savage B.D., Sembach K.R., 1996, ARAA 34, 279
Schilke P., Walmsley C.M., Pineau des Forêts G., Flower D.R., 1997 A&A 321, 293
Sivan J.P. 1974, A&AS 16, 163
Snow T.P., Lamers H.J.G.L.M., Lindholm D.M., ODell A.P., 1994, ApJS 95, 163-299
Sofia U.J., Cardelli J.A., Savage B.D., 1994, ApJ 430, 650
Spitzer L., & Fitzpatrick E., 1993, ApJ 409, 299
Trapero J., Welty D.E., Hobbs L.M., et al., 1996, ApJ. 468, 290
Whittet D.C.B., Prusti T., Franco G.A.P., et al., 1997, A&A, in press

This article was processed by the author using Springer-Verlag LaTeX A&A style file *L-AA* version 3.